DESY seminar talk, June 20, 2005

First Observation of Laser-Driven Particle Acceleration in a Semi-Infinite Vacuum Space

T. Plettner, R.L. Byer
E.L. Ginzton Laboratories, Stanford University

E. Colby, B. Cowan, C.M. Sears, R.H. Siemann, J.E. Spencer
ARDB, SLAC

Contents of the presentation

Motivation

historical trend of high energy physics experiments

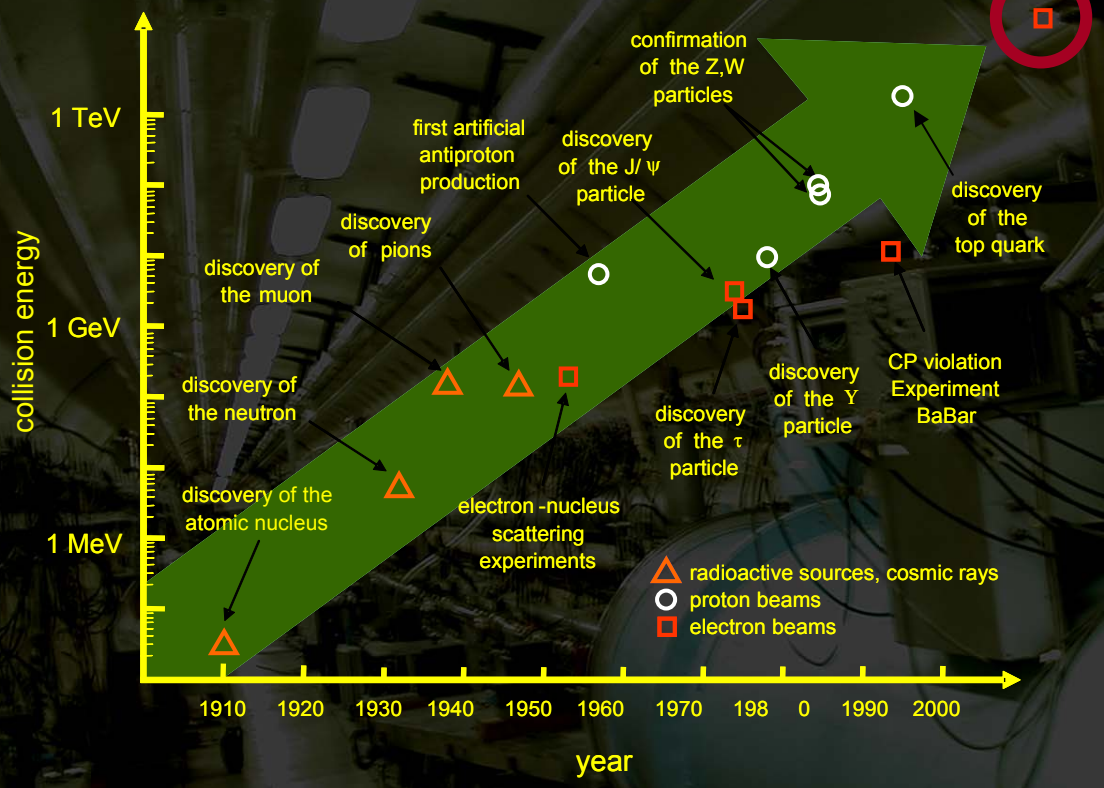

Future TeV e^+e^- collision experiments

explore new accelerator technologies capable of

- substantial improvement of energy gradients
  50 MeV/m → 1 GeV/m
- energy-scalable
- high luminosities at collision
- improved energy efficiency
- reliable and cost-effective technology

Laser driven particle acceleration in vacuum

Characteristics

- Crossing laser beams in vacuum
  - Longitudinal electric field of the laser pattern responsible for particle acceleration
- Dielectric accelerator structure
  - ~ 1 J/cm^2 damage threshold with ultra-short near IR lasers
  - with 100 fsec pulses peak fields of 10 GV/m possible
  - a 1 GeV/m gradient structure is possible[1]
- The acceleration is linear
  - we are interested in a linear acceleration process $G \sim E_{||}$
- The electrons stay in vacuum
  - no beam deterioration from scattering with matter

conceptual idea

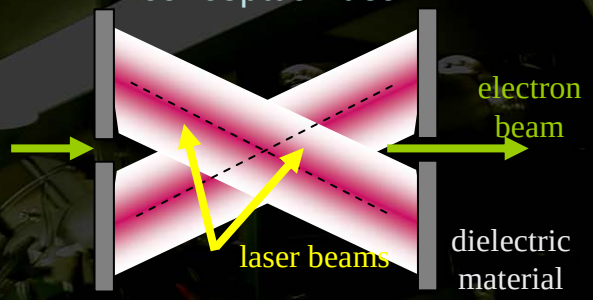

laser damage threshold

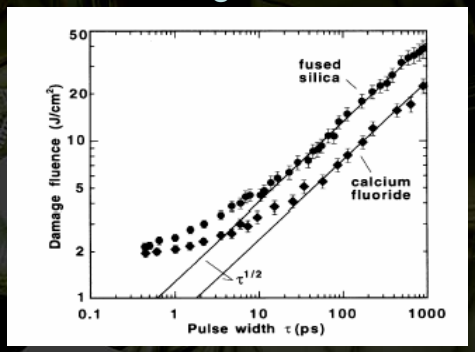

Stuart, et. al,, Phys Rev. Lett. Vol 74, No 12 p. 2248 (1995)

proposed 1 GeV/m structure

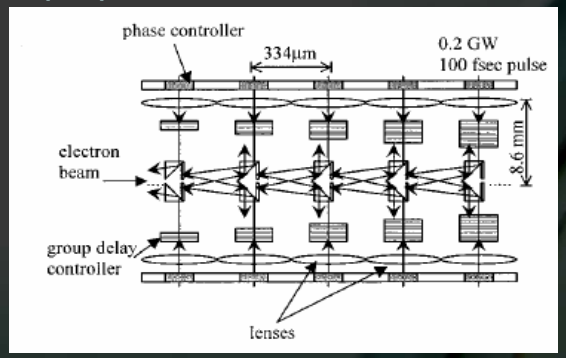

Y.C. Huang, et al, Appl. Phys. Lett. 68 (6) (1996) 753.

The basic physics concept

Example: Longitudinal electric field from crossed laser beams*

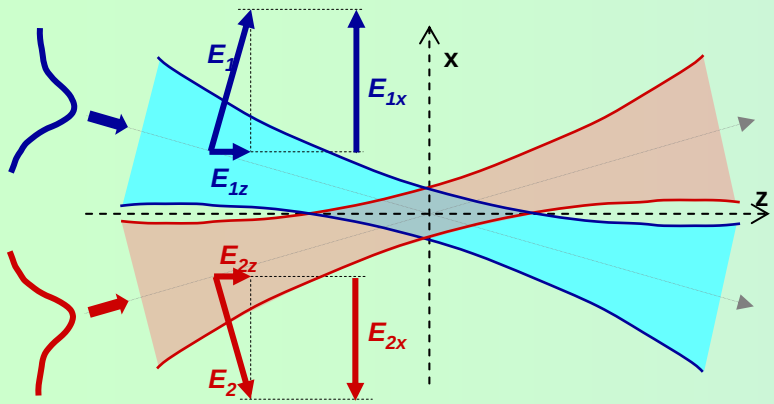

$$E_z = -\underbrace{\frac{2E_0 \sin\theta}{(1+\hat{z}^2\cos^2\theta)^{3/2}} \exp\left[-\frac{\left(\hat{z}/\theta_d\right)^2 \sin^2\theta}{1+\hat{z}^2\cos^2\theta}\right]}_{\text{Magnitude}} \times \underbrace{\cos\psi_t}_{\text{Phase}}$$

$$\psi_t = \underbrace{k\cdot z\cdot\cos\theta - \omega\cdot t}_{\text{Plane Wave Phase}} + \underbrace{\frac{\hat{z}^3\cos^3\theta\cdot\tan^2\theta}{\theta_d^{\,2}\left(1+\hat{z}^2\cos^2\theta\right)}}_{\text{Math}} \underbrace{-2\cdot\tan^{-1}\left(\hat{z}\cos\theta\right)+\phi_0}_{\text{Gouy Phase}}$$

$$U(z) = \int_{z_0}^{z} E_z(z')dz'$$

†P. Sprangle, E. Esarey, J. Krall, A. Ting, Laser Acceleration of Electrons in Vacuum, Optics Comm. 124 (1996) 69

Plot of the longitudinal E-field

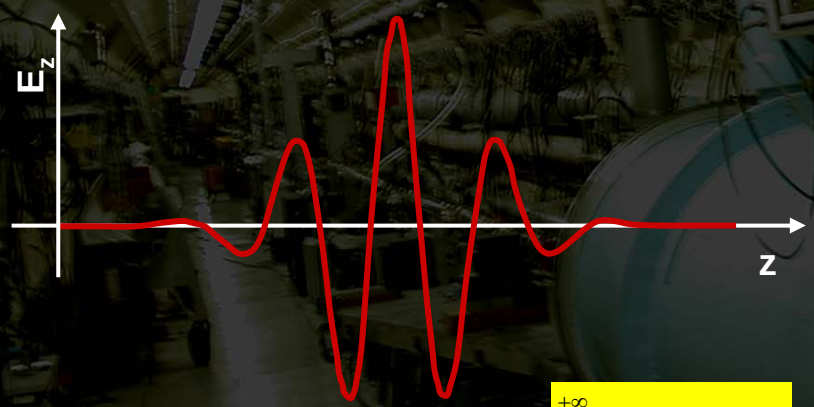

The Lawson-Woodward Theorem

$$\int_{-\infty}^{+\infty} E_z(z')dz' = 0$$

Limit the laser-electron interaction

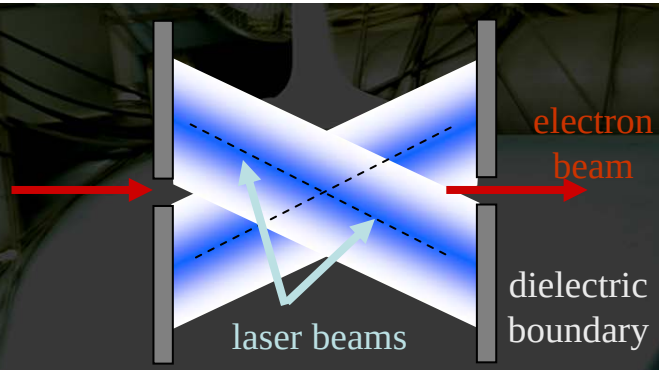

$$\int_{z_1}^{z_2} E_z(z')dz' \neq 0$$

*For an alternate picture of particle acceleration see Z. Huang, G. Stupakov, M. Solotorev, "Calculation and optimization of laser acceleration in vacuum", Phys. Rev. ST AB 7 011302 (2004)

The SCA-FEL Facility

HEPL beam parameters	
Beam Energy	~30 MeV
$T_{electron}$	~2 psec
Charge per bunch	~5 pC
Energy spread	~20 keV
λ_{laser}	800 nm
E_{laser}	1 mJ/pulse

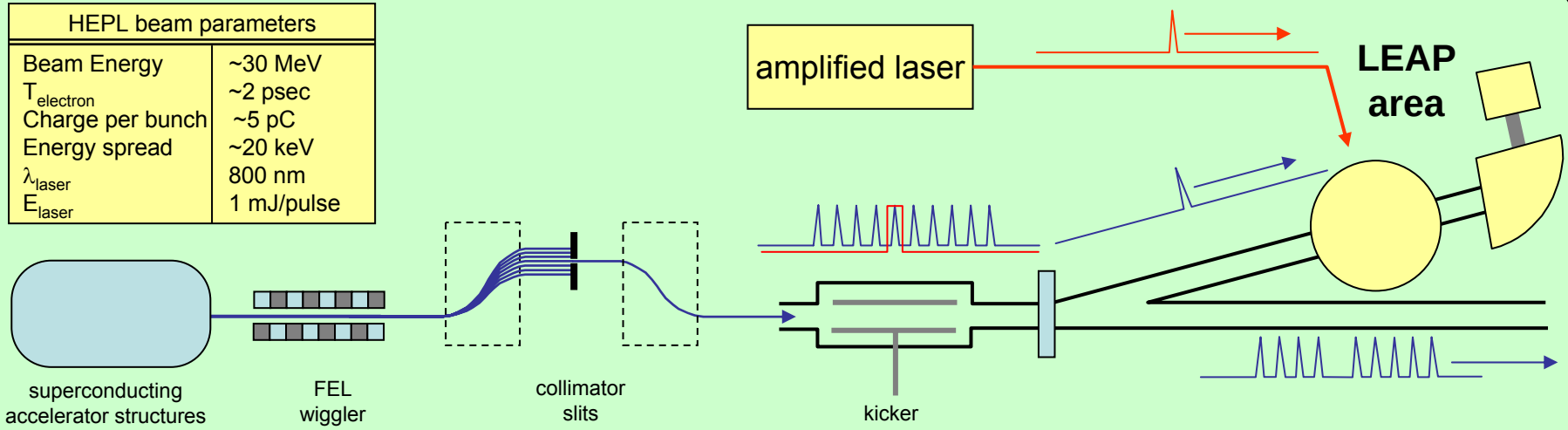

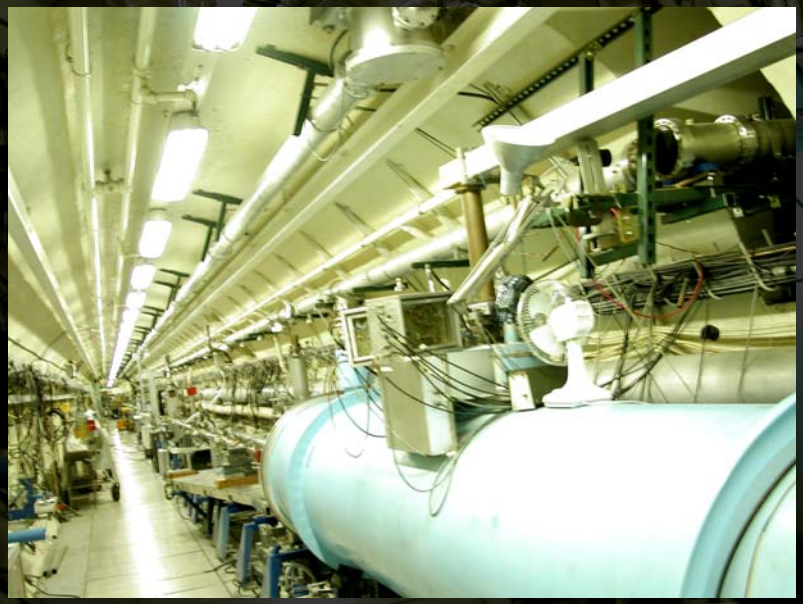

Main advantages
- Convenience of location
- Low beam energy spread from the superconducting accelerator

Experiment is being moved to the NLCTA at SLAC
- dedicated accelerator test facility
- more possibilities for upgrades and expansions
- 60 MeV electron beam
- no electron macro pulse structure

Contents of the presentation

The LEAP experiment setup

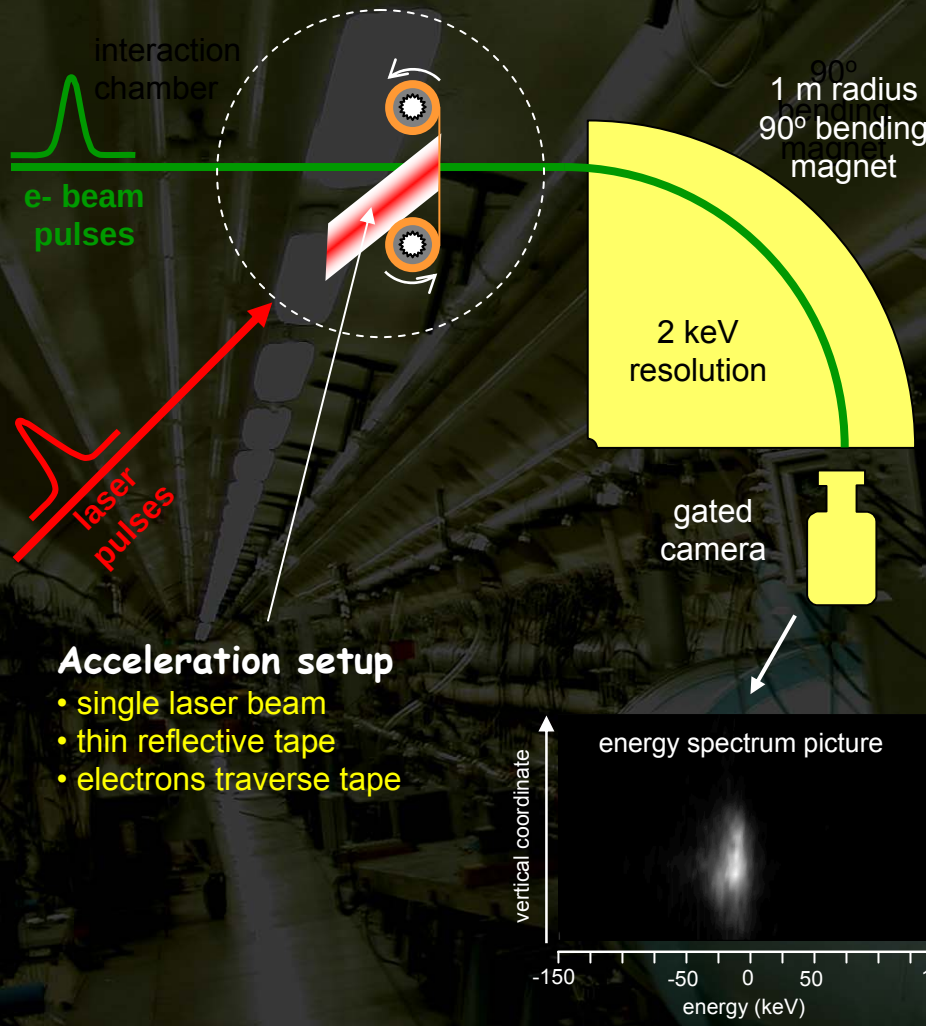

Acceleration setup

- single laser beam
- thin reflective tape
- electrons traverse tape

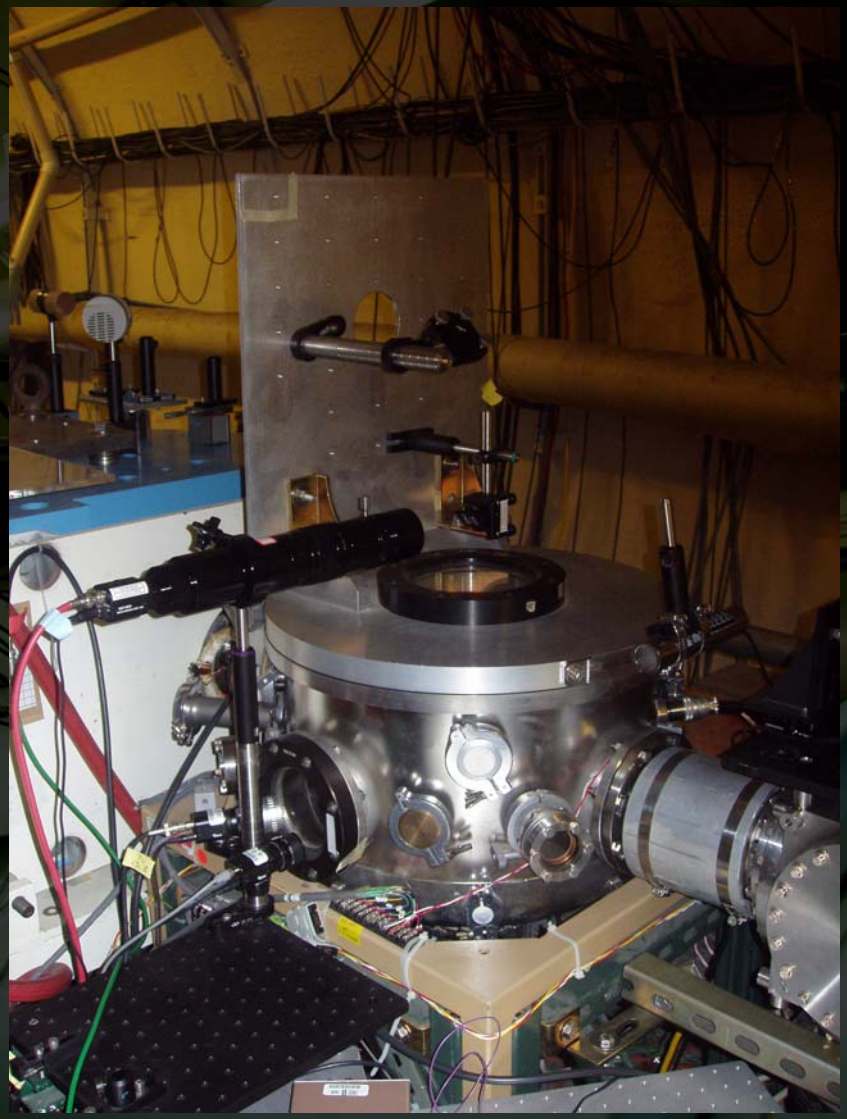

Problems with the old LEAP cell

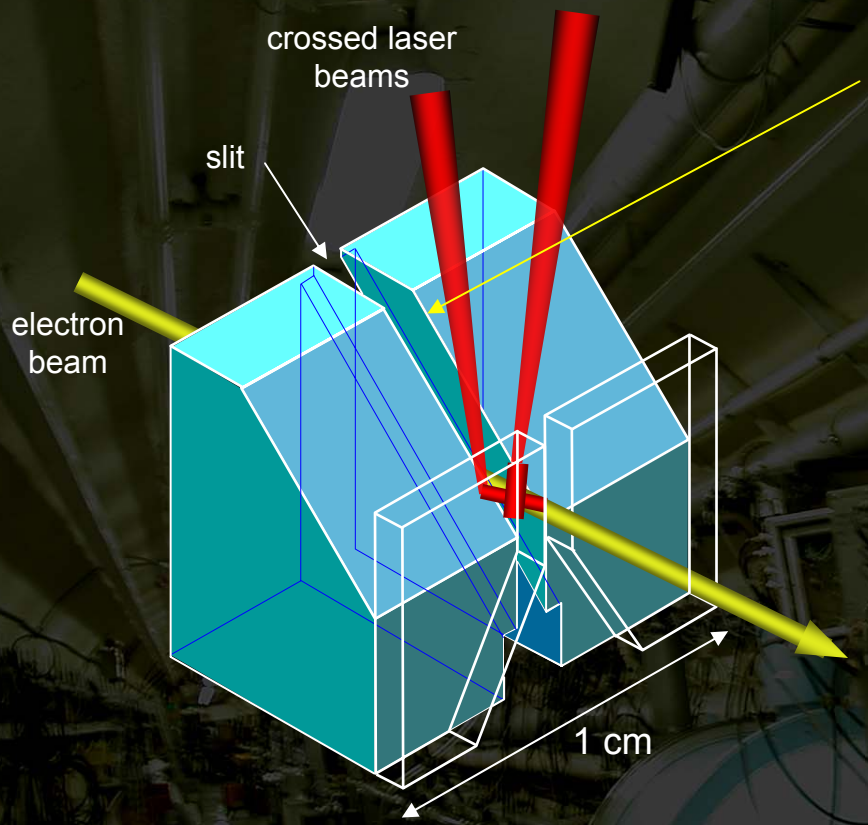

- **HR coated fused silica with sharp edges in vacuum**
  → reduction of laser damage threshold to ~ ¼ J/cm^2
  → max. energy gain of ~20 keV

- **moving part of accelerator cell for variable slit**
  → internal alignment uncertainty once in operation
  → very difficult e-beam alignment (heavy loss of beam through a 10 micron slit
  → poor transmission through the 10 μm slit

- **crossed laser beams**
  → difficult alignment inside the cell space
  → optical phase uncertainty

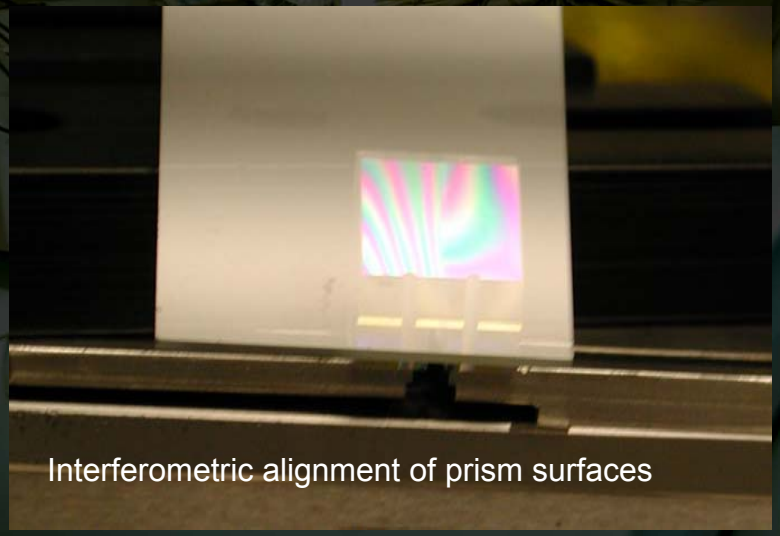

Interferometric alignment of prism surfaces

The simplified acceleration geometry and the disposable boundary

Improve on the very weak expected effect

1. **Damage threshold**
   - ignore it!
   - devise a "disposable" unit
   - materials retain their optical properties for a few picoseconds after a destructive laser pulse

Improve on
- Operation tolerances
- Poor reliability
- Ease of operation

2. **Cell geometry**
   - simplify to one semi-infinite boundary
   - make boundary thin enough to run e-beam through it
   - make boundary movable to present a new surface for each laser shot

3. **Crossed laser beams**
   - two laser beams too difficult? → eliminate one of them
   - no more optical phase uncertainty problems negligible transverse deflection forces

Conceptual drawing of the improved setup

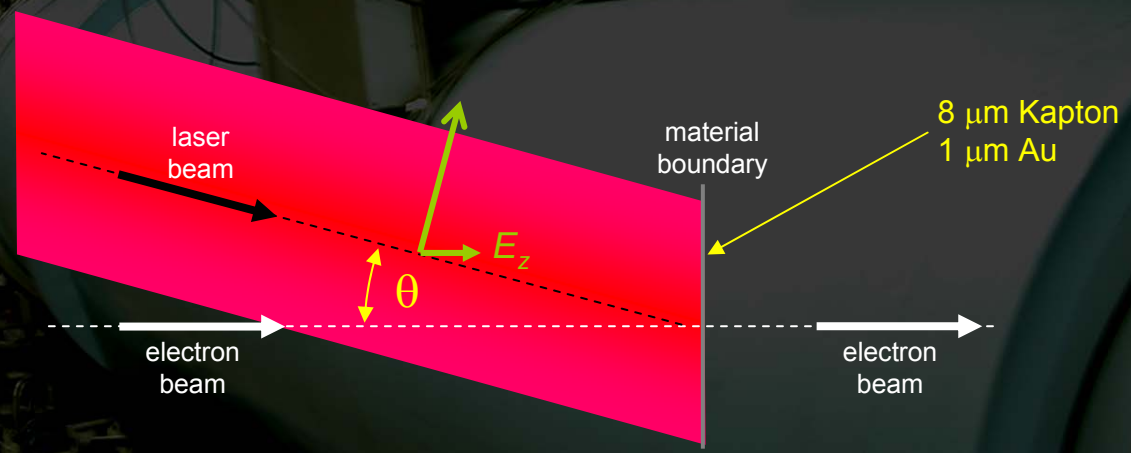

The reflective boundary tape drive

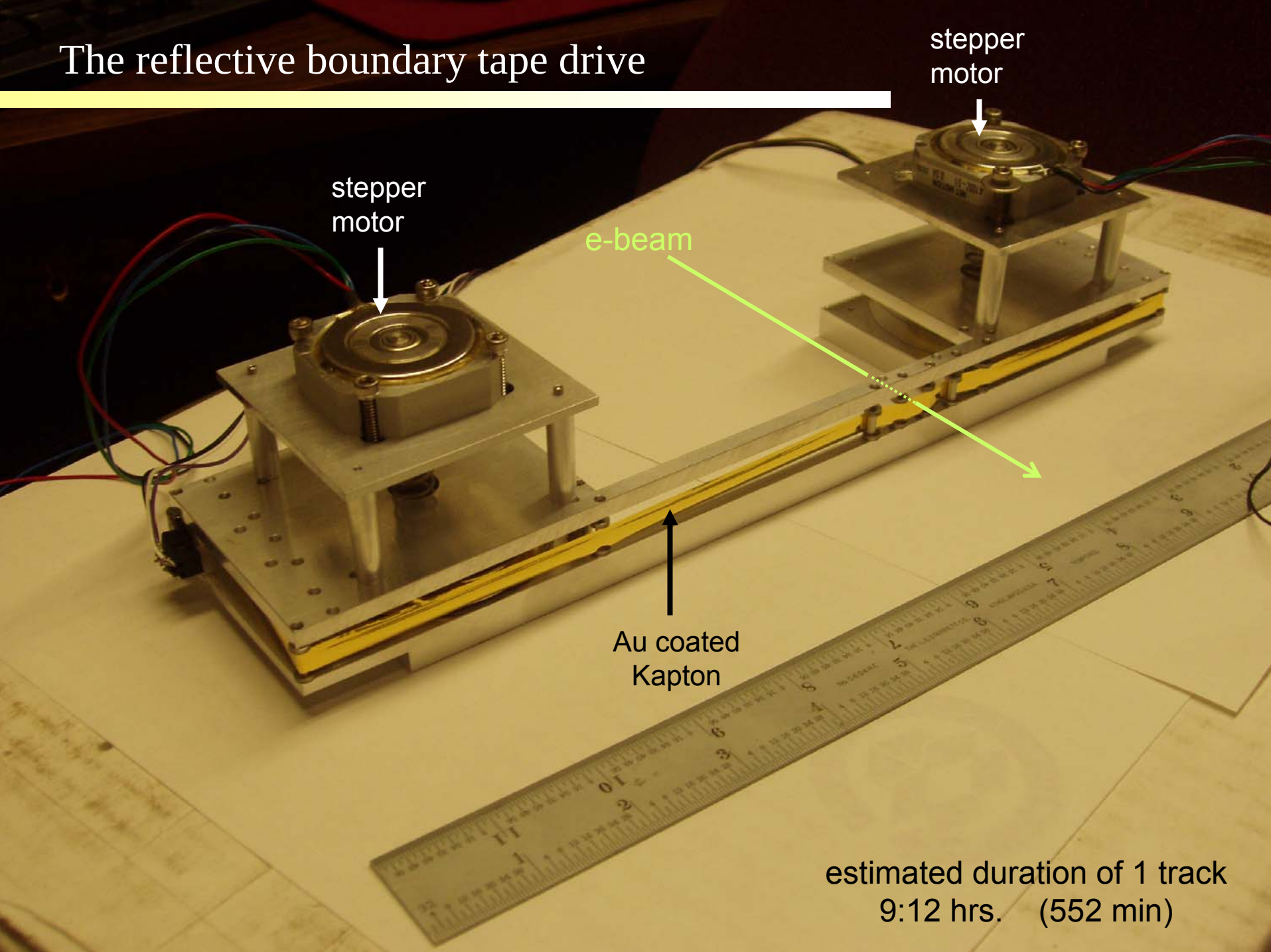

estimated duration of 1 track
9:12 hrs. (552 min)

Dual IFEL-ITR experiment operation

Use the IFEL as a psec-resolution timing diagnostic

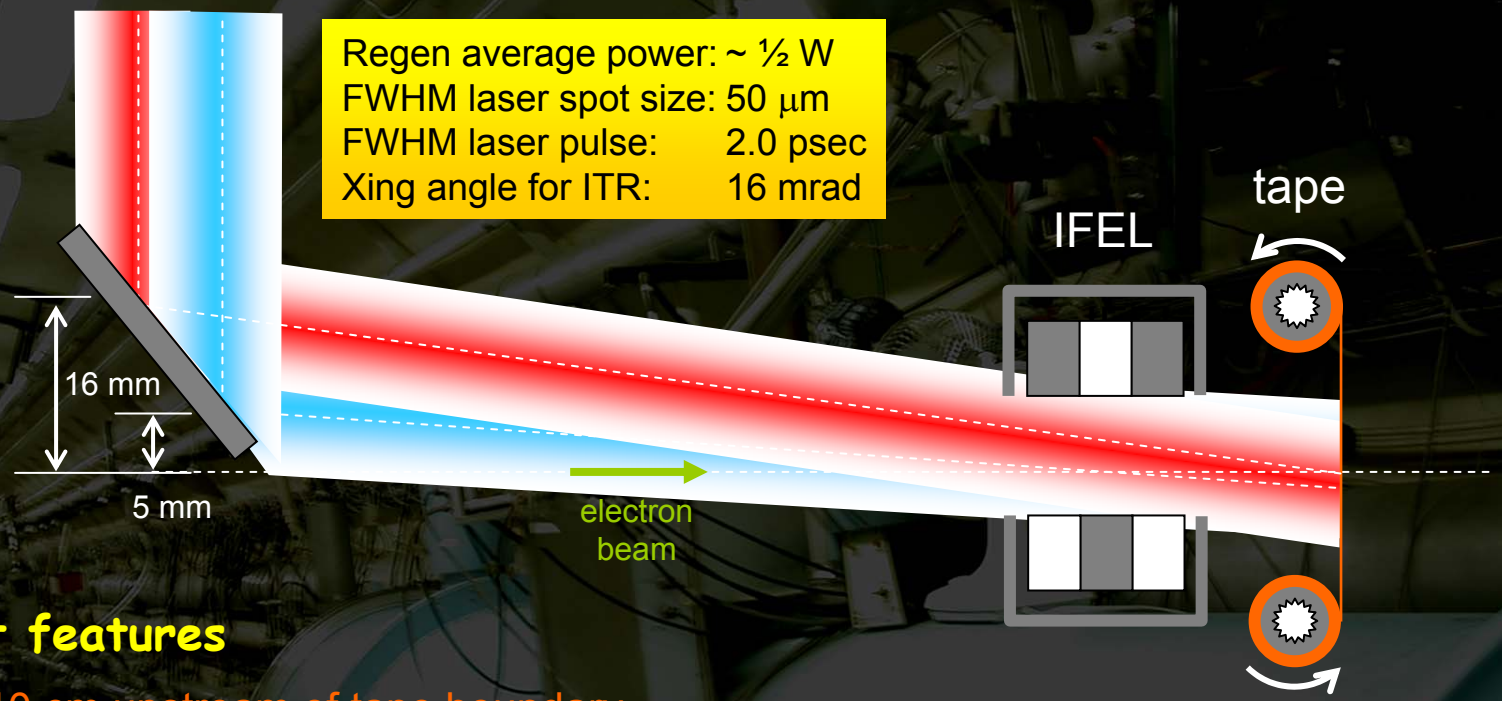

Important features

- IFEL ~10 cm upstream of tape boundary
- laser and electron beams cannot be simultaneously aligned for both the IFEL and the tape
- IFEL and ITR timing conditions are almost identical
- The IFEL produces a larger and easier to detect signal

See publication by C.M. Sears et al, "High Harmonic IFEL at 800 nm“ (TPAE029)

Top view of breadboard

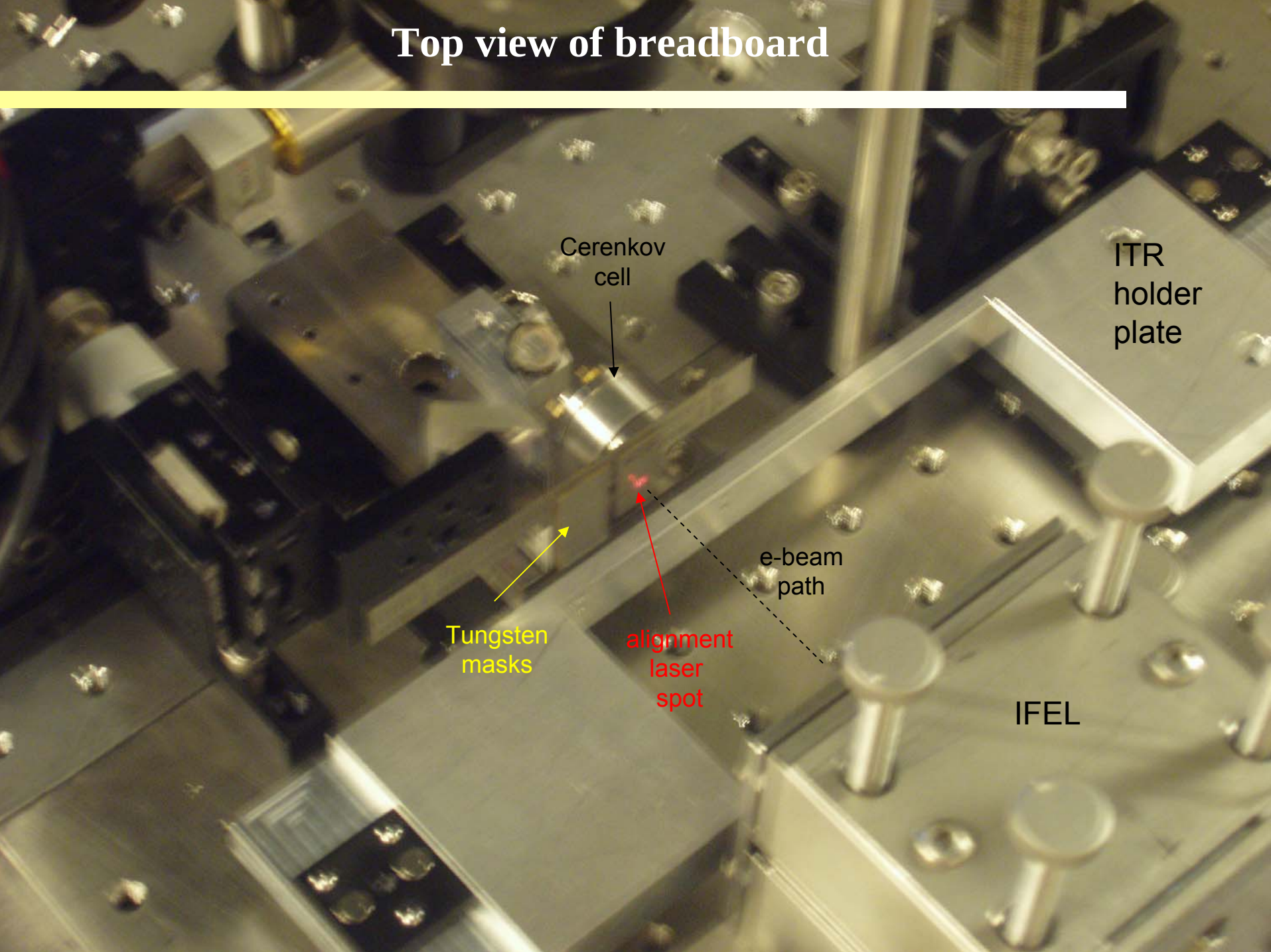

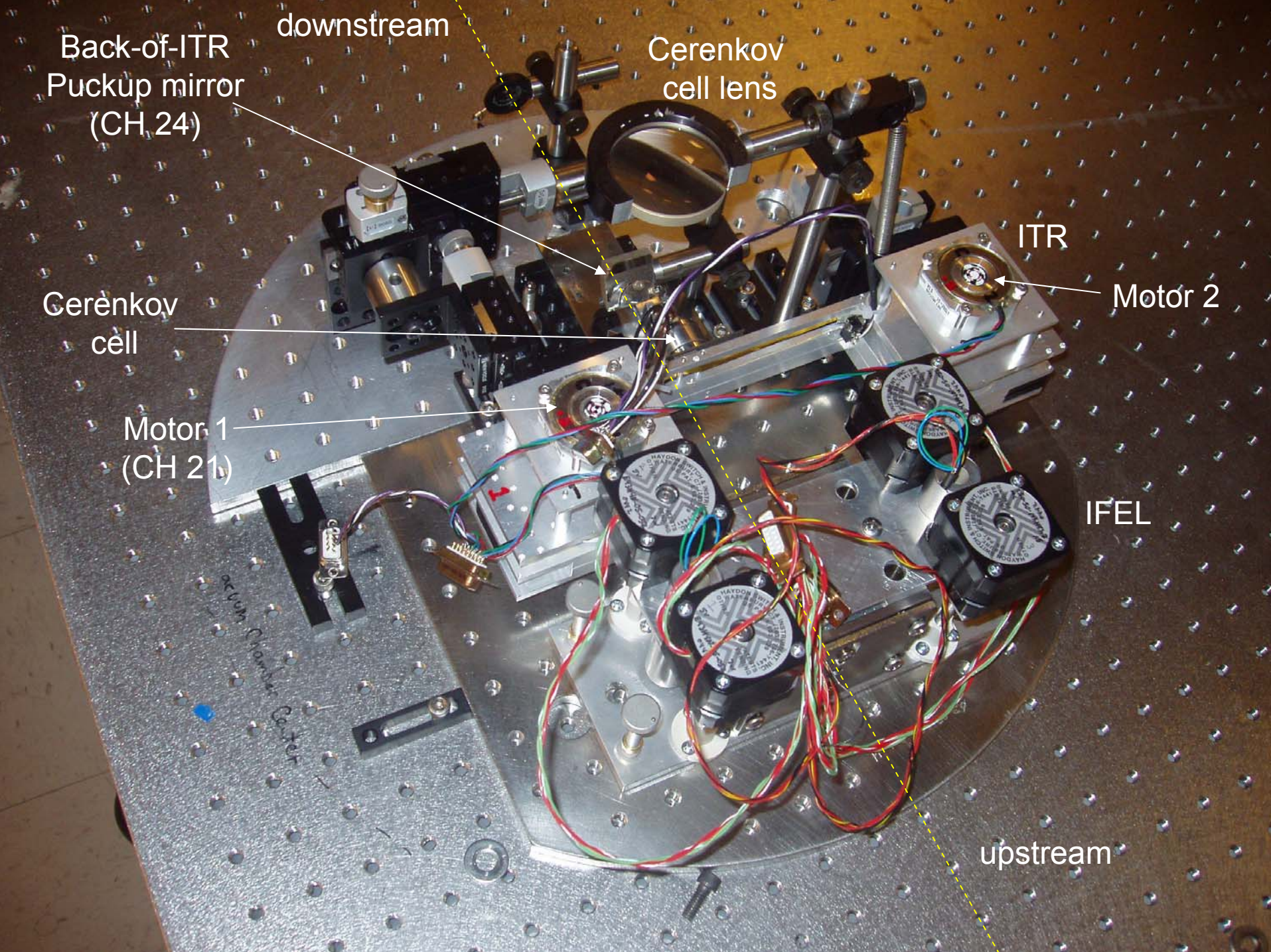
downstream
Back-of-ITR
Puckup mirror
(CH 24)
Cerenkov
cell lens
ITR
Motor 2
Cerenkov
cell
Motor 1
(CH 21)
IFEL
upstream

Contents of the presentation

Expected observations at the energy spectrometer

Electrons are not optically bunched

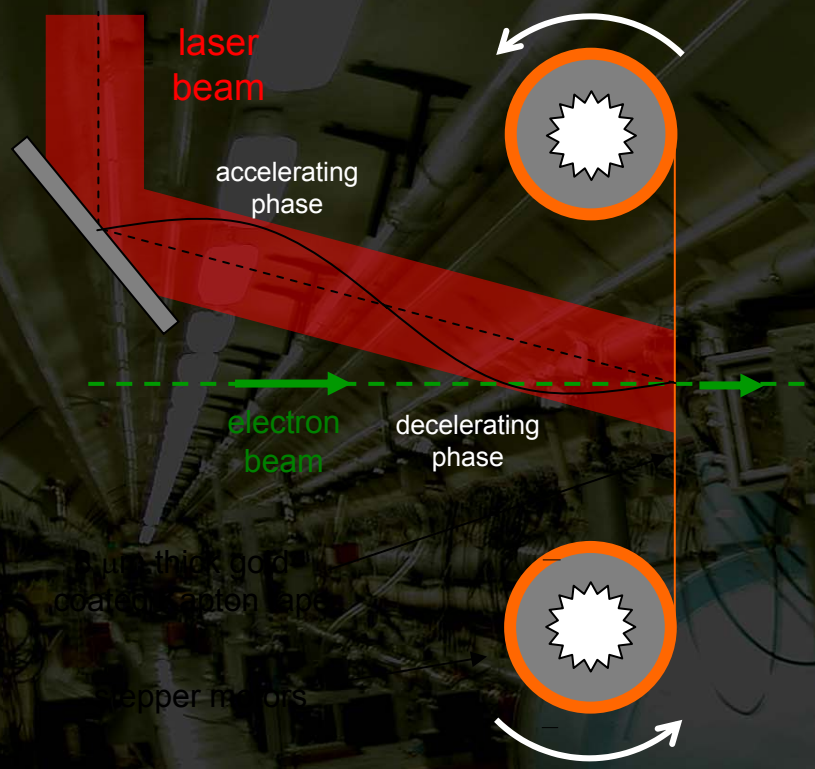

Electrons are distributed evenly over all the laser optical phases

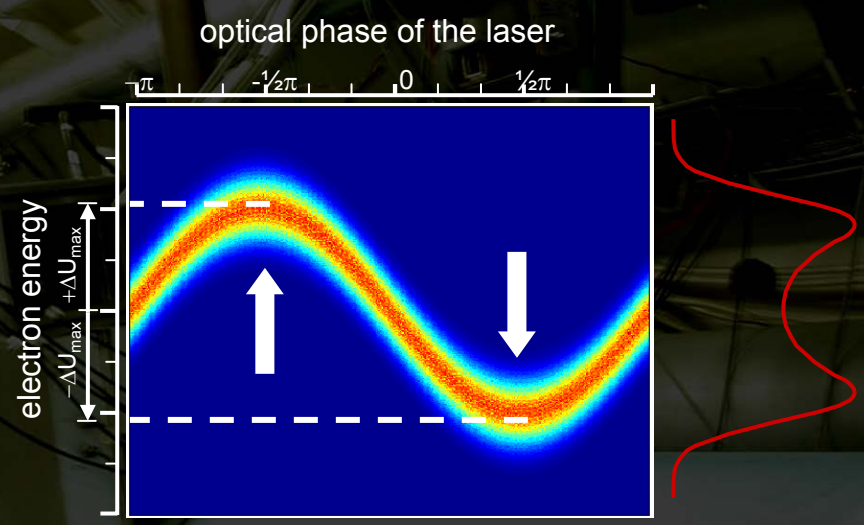

We expect to observe a broadening of the initial energy spread of the electron beam that is related to the modulation strength of the laser

Data acquisition

Data was taken as laser time scans

- timing of laser shots scanned over a 20-30 psec timing window
- laser was randomly toggled on and off
- we look for changes of the energy width between laser-on and laser-off data

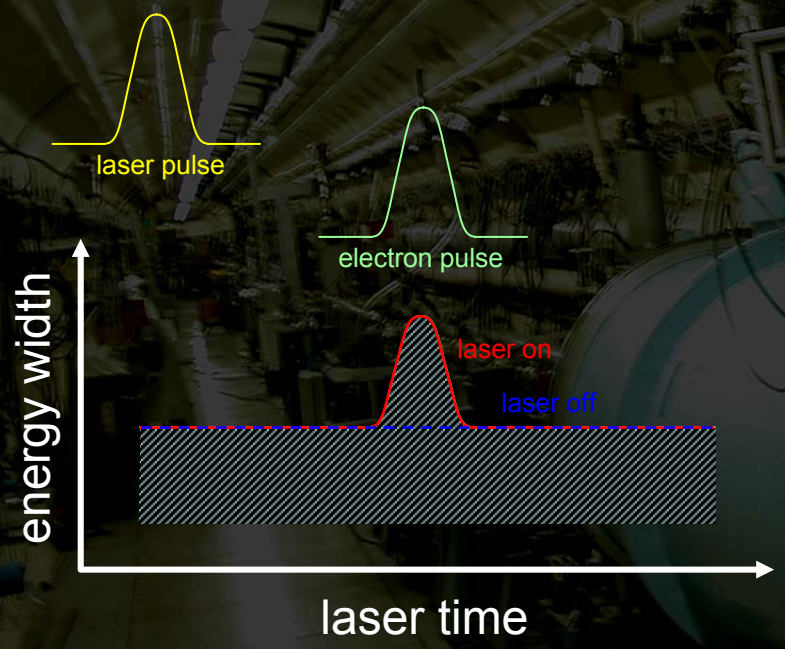

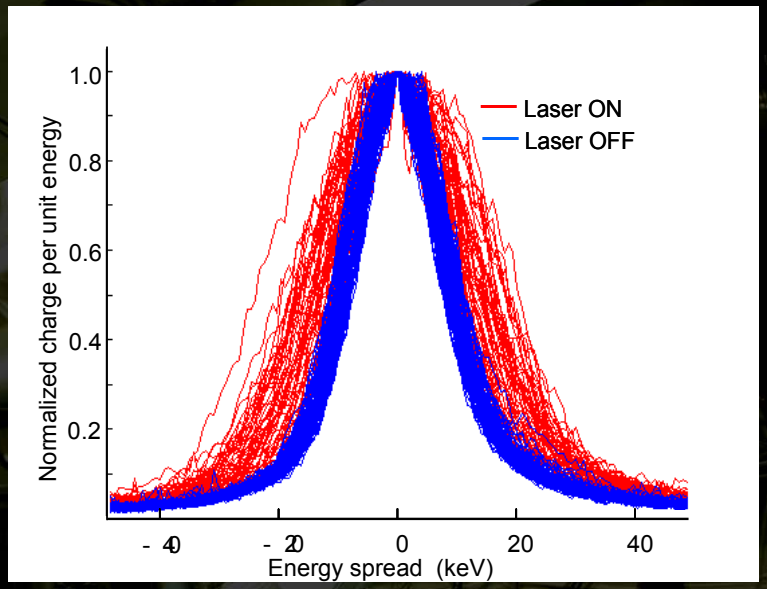

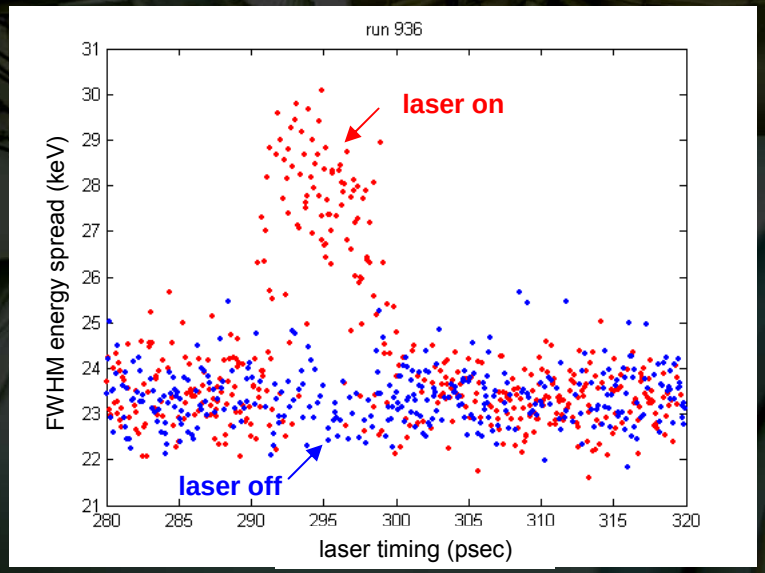

Expected dependence of the laser-driven energy modulation

effects we studied during the accelerator run

1. The Lawson-Woodward Theorem
2. Laser peak electric field
3. Laser polarization
4. Laser crossing angle

Expected dependences

Numerical integration of the longitudinal electric field along the e-beam trajectory

$$U = \int_{-\infty}^{0} e \cdot E_z(z')dz'$$

Laser angle

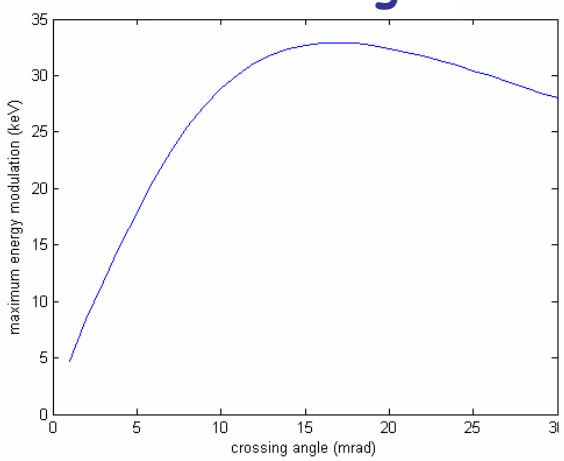

$$|U| \propto |\sin\alpha \cdot Z_{slippage}|$$

Laser electric field

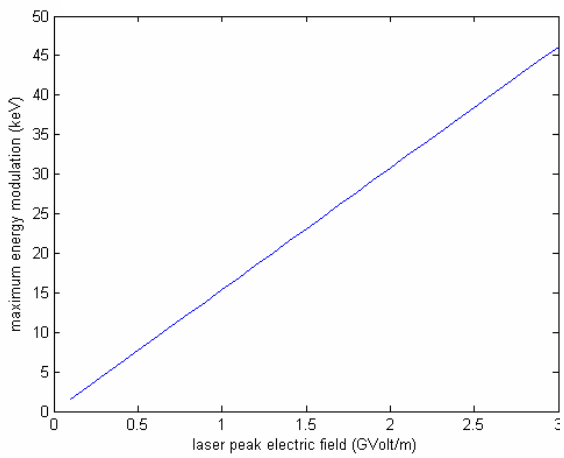

$$|U| \propto |E|_{laser}$$

Laser polarization

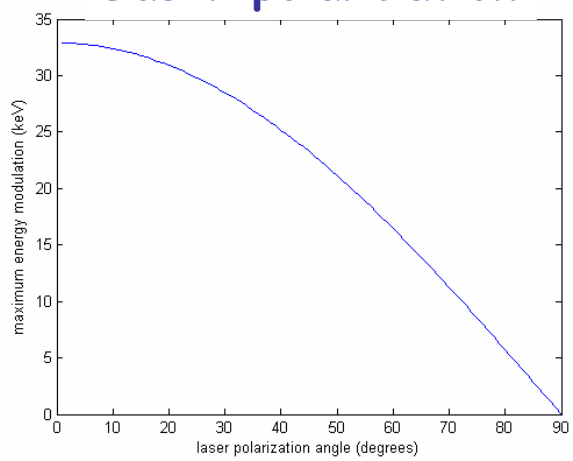

$$|U| \propto |\cos\phi|$$

Confirmation of the Lawson-Woodward Theorem

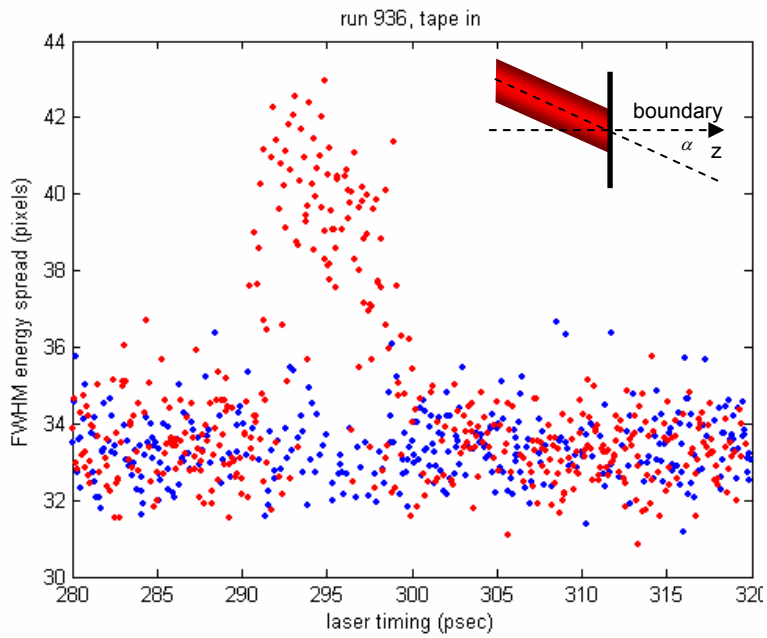

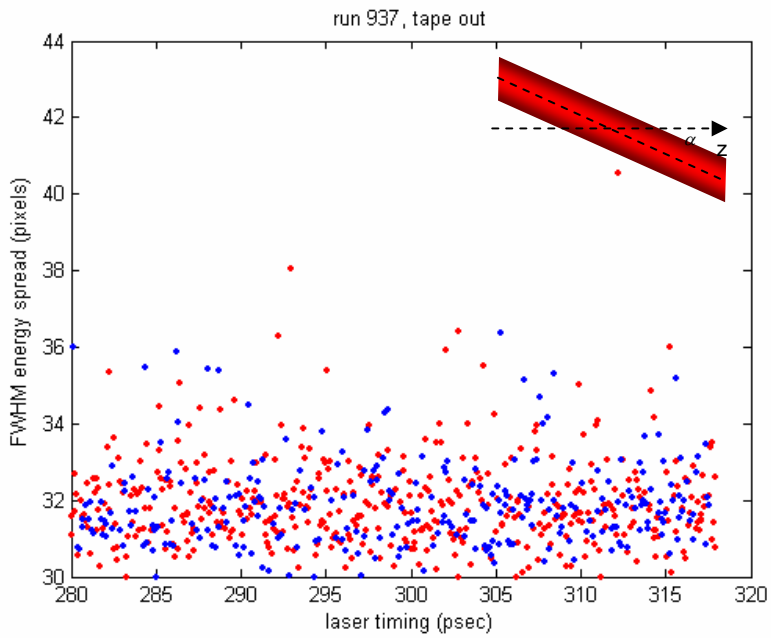

This confirms:

1. The Lawson-Woodward Theorem
2. No interaction from the IFEL

Laser electric field strength dependence

$$|U| \propto |E|_{laser}$$

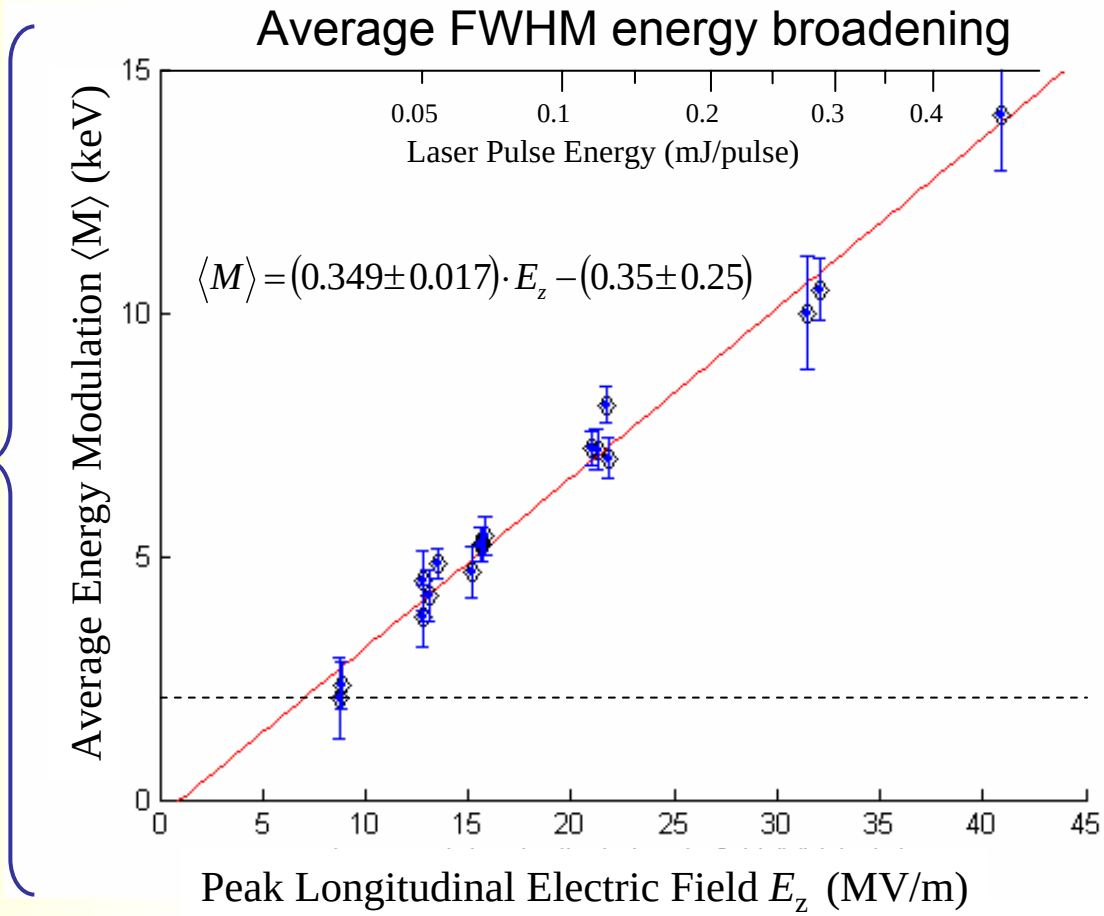

Laser polarization angle dependence

$$|U| \propto |\cos\phi|$$

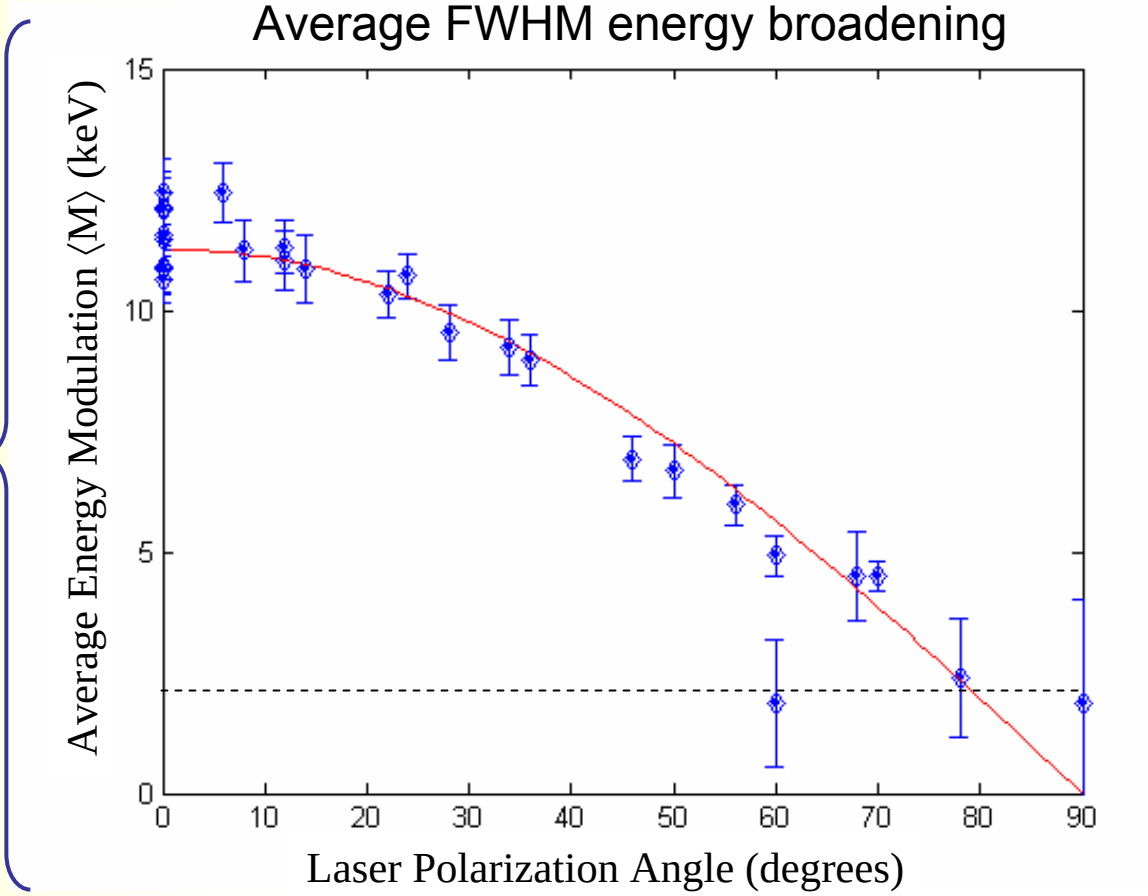

Laser crossing angle dependence

qualitatively

$|U| \propto \alpha$ for small α

$|U| \sim$ const. for bigger α

ideally

$$|U| \propto |\sin\alpha \cdot Z_{slippage}|$$

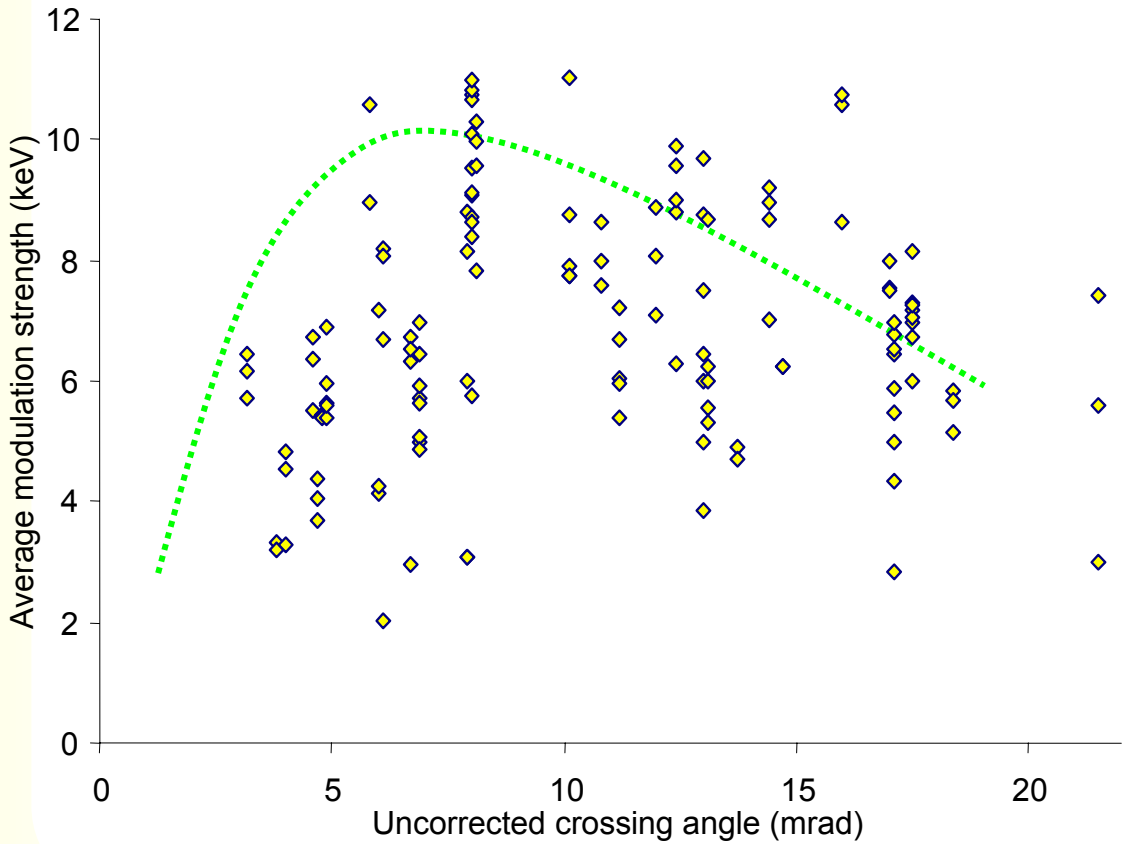

- measurement required realigning of laser and electron beam
- data set extended over several days
- electron beam conditions varied over this period of time

Did we do a modified plasma wakefield accelerator experiment?

From a plasma wakefield acceleration I would expect…

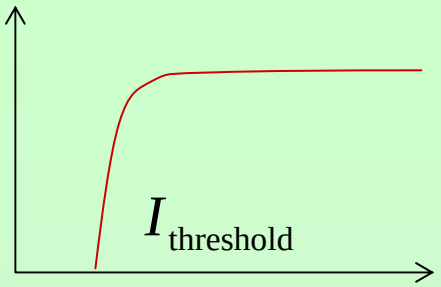

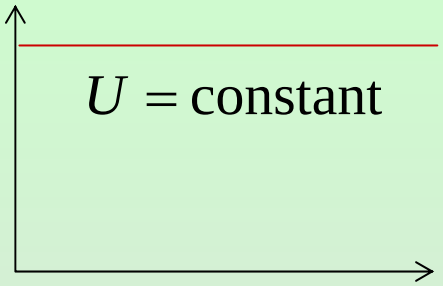

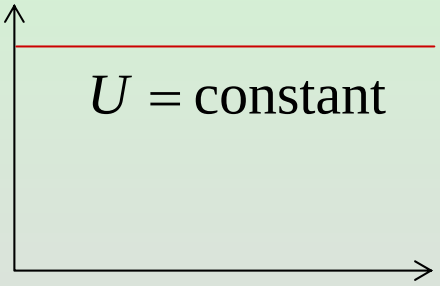

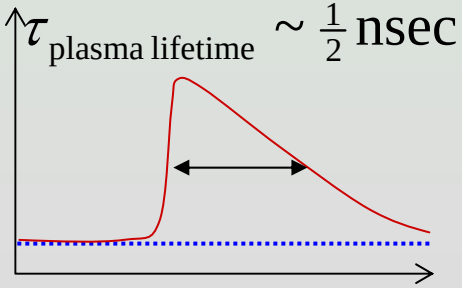

But I observe…

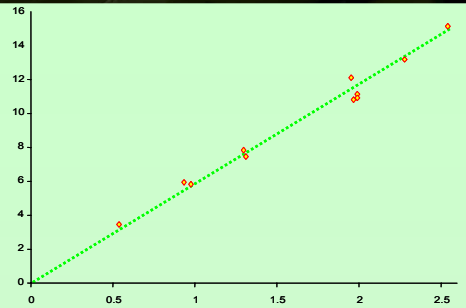

$$|U| \propto |E|_{laser}$$

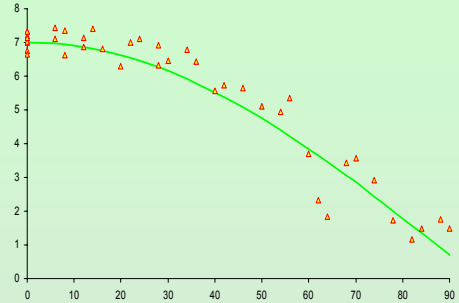

$$|U| \propto |\cos\phi|$$

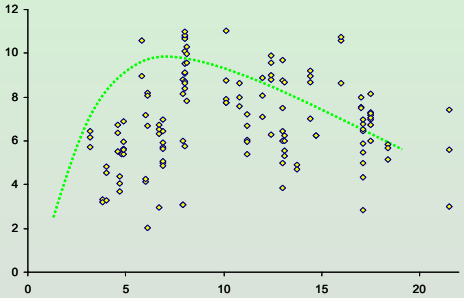

$$|U| \propto |\sin\alpha \cdot Z_{slippage}|$$

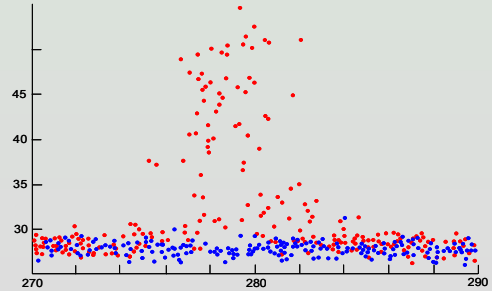

$$\tau_{\text{interaction}} \sim 5\,\text{psec}$$

Contents of the presentation

Phase I: Single Cell Laser Acceleration

This is the continuation of the LEAP experiment

objectives

1. repetition of the tape boundary experiment

verify

- laser power, polarization &crossing angle
- boundary type
- reflected laser spot quality

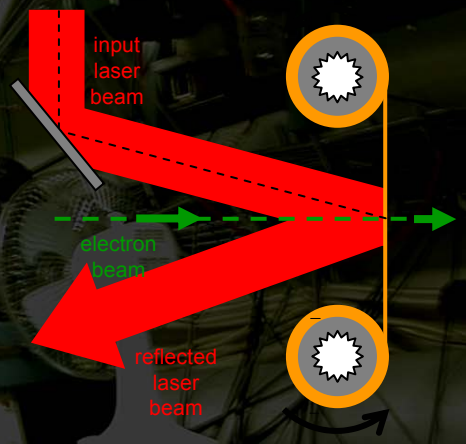

2. switch to a dielectric single cell structure

verify

- laser-electron interaction length
- laser crossing angle
- accelerator aperture size
- tolerances of the cell

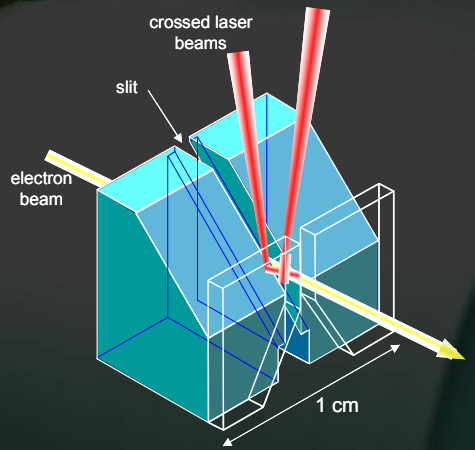

The E163 experiment

Phase II: Optical buncher – accelerator cell staged experiments

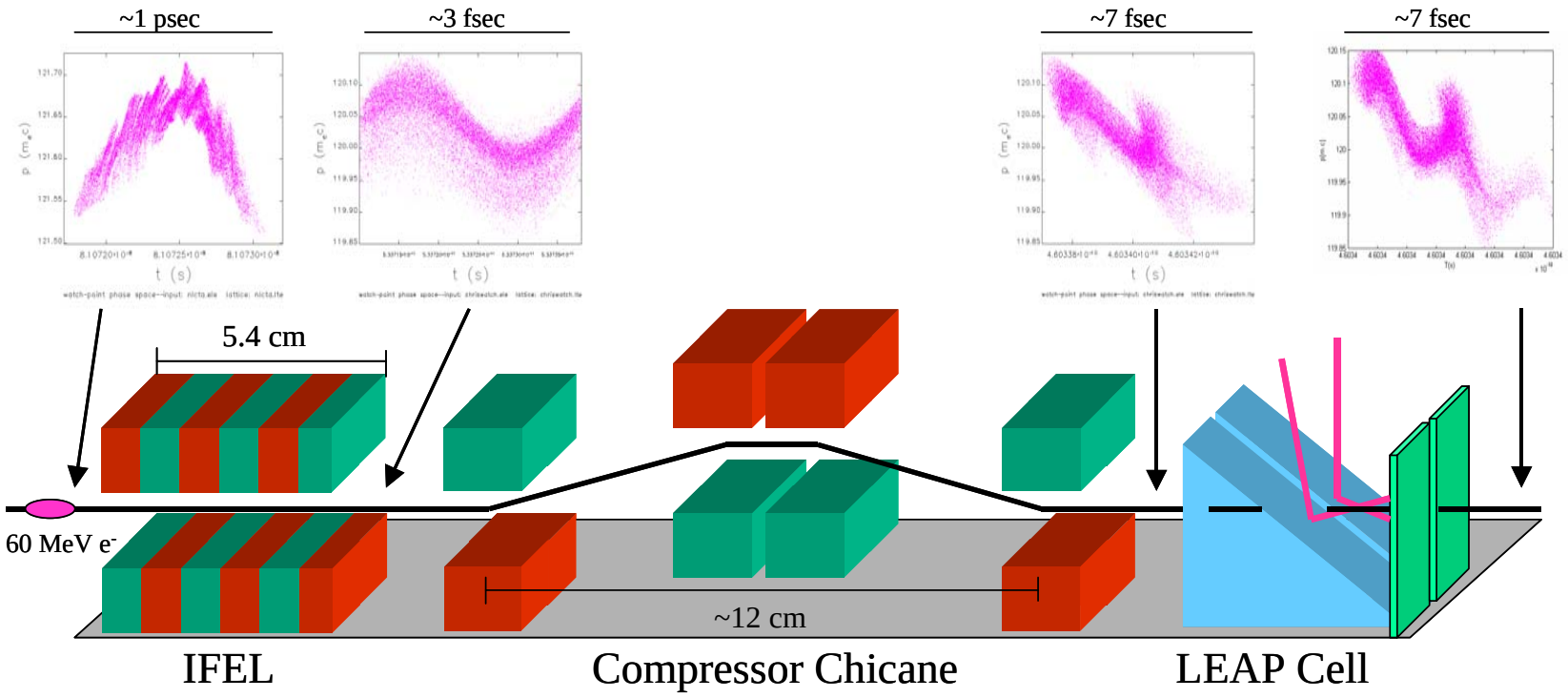

See publication by C.M. Sears et al, "High Harmonic IFEL at 800 nm“ (TPAE029)

The E163 experiment

Phase III: Guided-Mode Structures

(a)

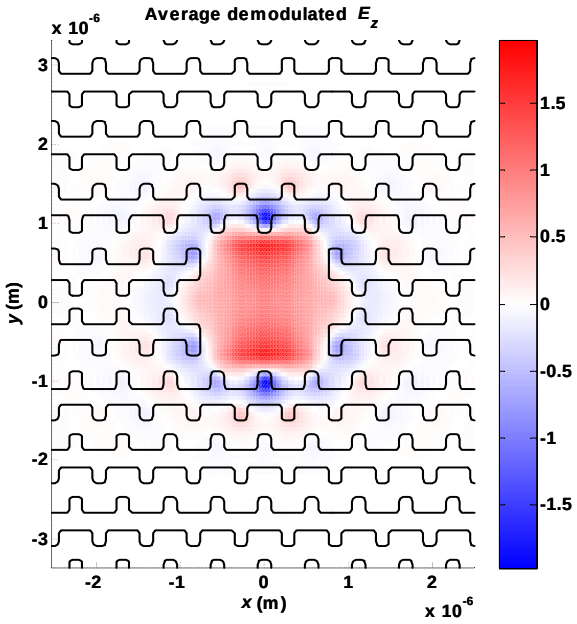

(b)

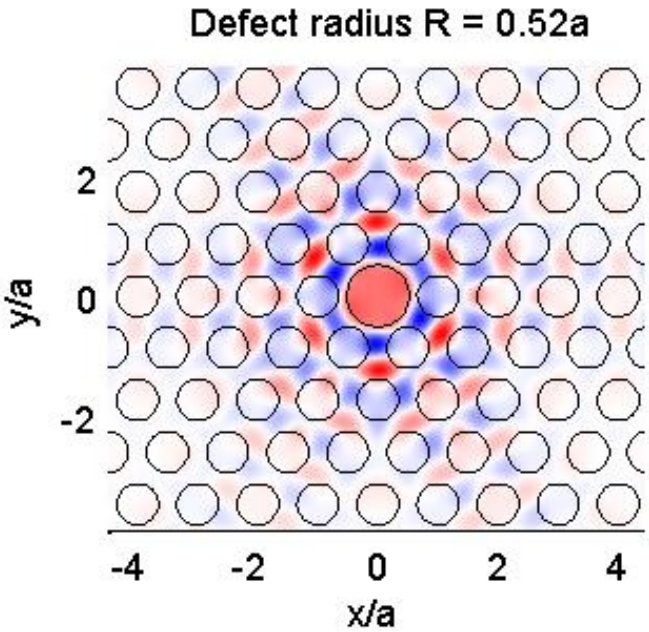

See publication by B. Cowan, “Photonic Crystal Laser-Driven Accelerator Structures” (TOPA010)

Summary

- **we have laser-accelerated electrons in vacuum**

  The laser wavelength was in the visible
  This was an energy-modulation experiment
  We employed a disposable boundary

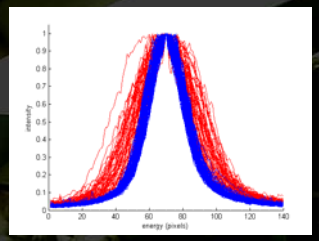

- **the effect is consistent with laser driven particle acceleration in vacuum**

  It follows the Lawson-Woodward theorem

  $U \leftrightarrow |E_{laser}|$

  $U \leftrightarrow |\cos \phi|$

  $U \leftrightarrow |\sin \alpha \cdot Z_{\text{slippage}}|$

- **with the successful IFEL operation we have already started phase II of E-163**

  The results from the IFEL alone are new

Acknowledgements

- The Department of Energy
- Mike Hennessy (ES II)
- Todd Smith (HEPL)
- The SCA personnel; George Marcus M. Galt, B. Armstrong, T. Kimura, D. Keegan, R.Swent, A. Schwettman, J. Haydon
- R. Route, V. Drew
- B. Noble, D. Walz (ARDB, SLAC)
- Y.C. Huang, C. Barnes, S. Waldman, J. Wisdom

Laser and Particle Guiding Micro-Elements for Particle Accelerators*

R.Gaume,T.Plettner, J. Wisdom, *Stanford University*
J. Spencer, *SLAC*

Objective

Develop materials and micro-machining technologies for integrated micro-elements for laser driven particle accelerators. Our focus is on magnetic and optical micro-elements.

Summary of Work

We have focused on micromachining techniques on silicon and have begun exploring ceramic materials as components for laser driven particle accelerator structures. In addition, we have carried out studies on radiation sensitivity of various candidate materials.

Desired Properties of the materials

- high laser damage threshold
- radiation resistant
- high melting point
- good thermal conductivity
- optical transparency
- inexpensive, machineable

radiation sensitivity

example

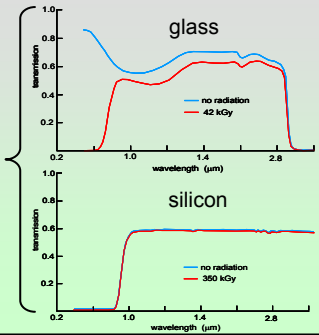

*E. Colby, G. Lum, T. Plettner, J. Spencer, "Gamma Radiation Studies on Optical Materials", IEEE Trans. Nucl. Sci. Vol. 49, No. 6, p. 2857-2867 (2002)

Silicon micromachining

Advantages of Si

- advanced micromachining technology
- possibility for integrated electronic circuits
- optically transparent 1.5-10 μm
- abundant and inexpensive
- high index of refraction
- good heat conductor
- radiation resistant

Optical quality surfaces

mm-deep trenches

Sharp point-features

Problems

•limited geometry freedom with existing anisotropic etching techniques

•semiconductor:→ lower bandgap energy, easier multiphoton absorbtion and thus lower laser damage threshold

Ceramics micromachining

Advantages of ceramics

- possibility for magnetic and optical materials from compatible substrates
- macroscopically amorphous: no restricted geometry limitations
- potentially higher degree of purity and less defect sites
- enhanced flexibility in mixing of different materials
- do not require expensive crystal growth step
- typical substrates like YAG: larger bad gap
  - → also transparent at visible wavelengths
  - → higher laser damage threshold
  - → higher melting points

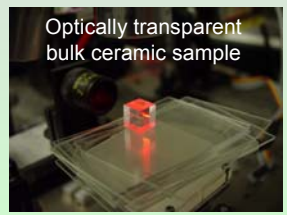

Optically transparent bulk ceramic sample

50 μm spacing pattern Imprinted with a Silicon preform

Challenges

- optical ceramics fabrication technology is a relatively new topic
- micromachining technology on ceramics to sub-μm resolution has not been developed.

*Supported by DOEW grants DE-FG03-97ER41276 and DE-AC02-76SF00515.

Optical Phase Locking of Modelocked Lasers for Particle Accelerators

Present accomplishments

- observed the comb offset from a commercial Ti:Sapphire modelocked laser
- isolated a comb offset error signal
- manipulated the comb offset with an electronic signal
- constructed and tested a balanced cross-correlator
- we are presently switching to a 1 mm Yb:glass fiber modelocked laser

Comb offset detection experiment

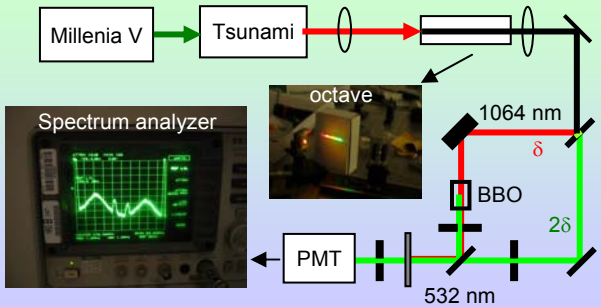

Beatnote detection circuitry

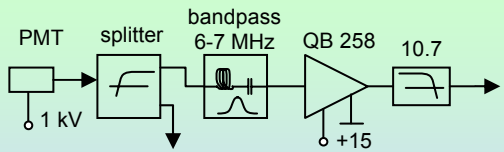

Two parameters for the control of the optical phase for modelocked lasers

Pulse envelope timing and carrier-to-envelope phase

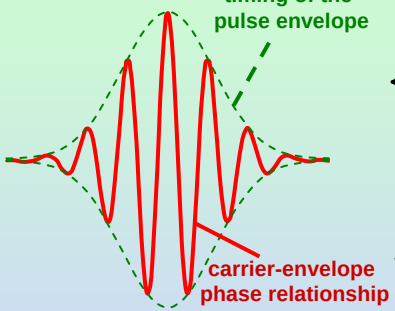

Timing detection and control to within a fraction of an optical cycle (1 opt. cycle ~ 3 fsec)

Balanced cross correlator technique (40° of optical phase)

Frequency comb stabilization techniques Requires one octave of bandwidth.

Time domain picture

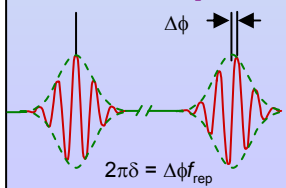

Frequency domain picture

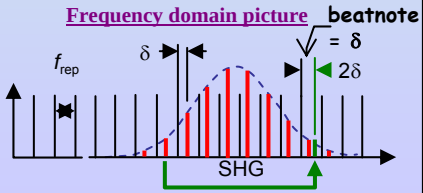

Comb Self referencing technique

Error signal generation

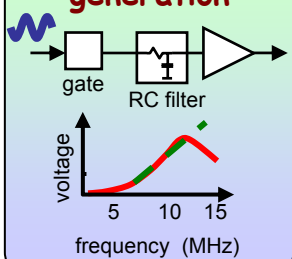

Comb offset control

Error signal into AOM controls pump power and dispersion of laser

AOM signal: 1.0 kHz, 0.2V square wave

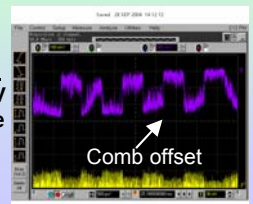

The balanced cross-correlator experiment

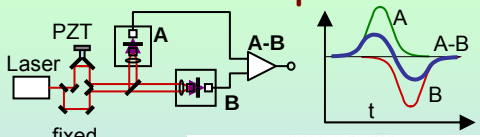

PZT delay

V_{pp} = 60 mV
t = 240 attosec

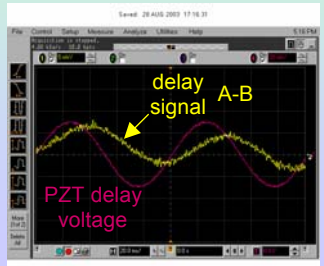

Future objectives

repeat these measurements with the fiber laser

- feedback the comb error signal and stabilize the comb offset of a single laser
- construct a second identical fiber laser
- synchronize the pulse envelopes of the lasers to sub-fsec with the balanced cross-corr. technique
- eliminate residual phase jitter with an external interferometer unit controlling a variable path delay (e.g. a PZT)

control the pulse envelope to ~40°

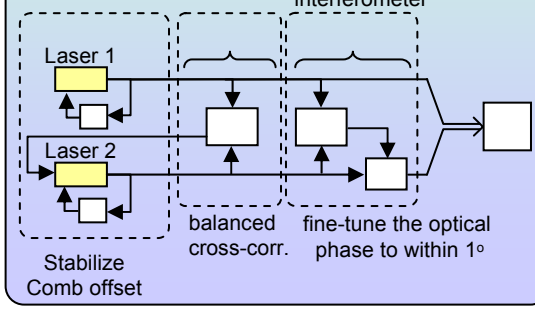

† Supported by DOEW grants DE-FG03-97ER41276 and DE-AC02-76SF00515.

Side Note on laser ablation dynamics

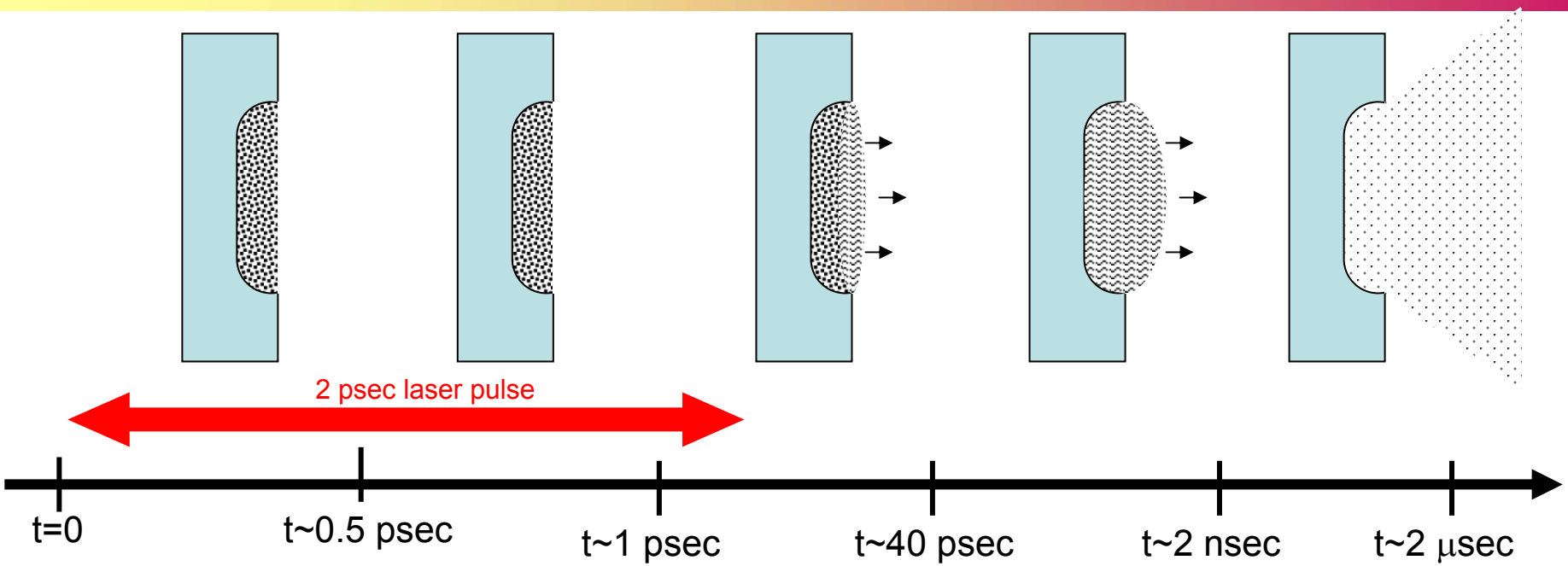

excitation stage

- excited solid
- formation of electron-hole pairs
- Renormalization of the band structure
- Change of the optical properties
- Reduction of the band gap

transition stage

- Transformation into a liquid sate
- ~100 nm layer of material with metallic properties

rarefaction wave

- Low-density shock wave traveling at the speed of sound of the material c~ 2500 m/sec

expansion phase

- Expansion of the ablation front

ejection phase

- Ejection of monomers and molecular clusters

$$N_e \sim 10^{22} / \text{cc.}$$

During the passage of the laser and the electron beam the surface of the tape is a metallic high reflector

http://www.ilp.physik.uni-essen.de/vonderLinde/Publikationen/ICONO98.pdf

laser ablation dynamics experiment

We measured reflectivity of 1st ablation reflected spot vs. laser pulse duration

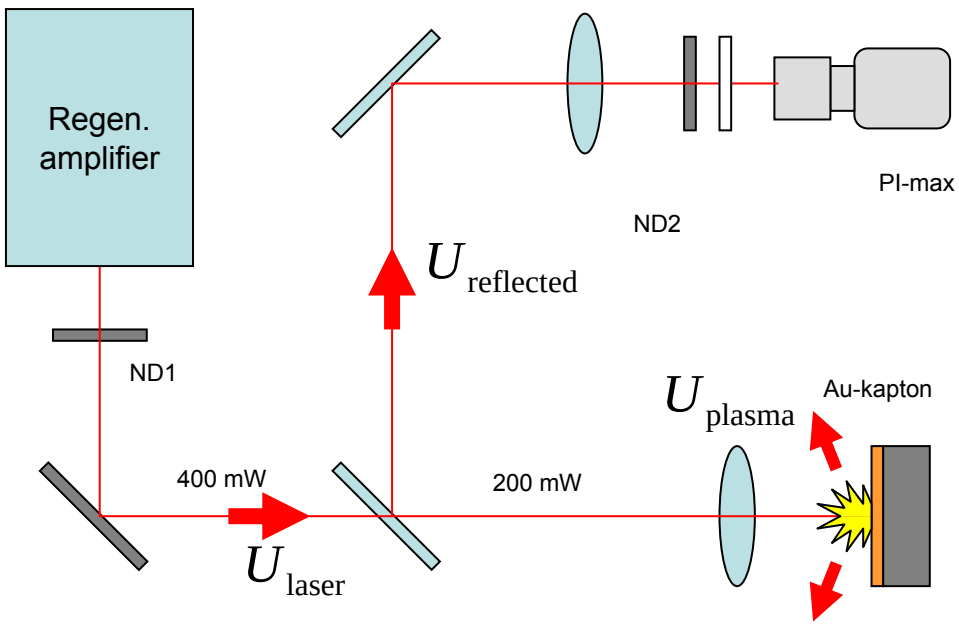

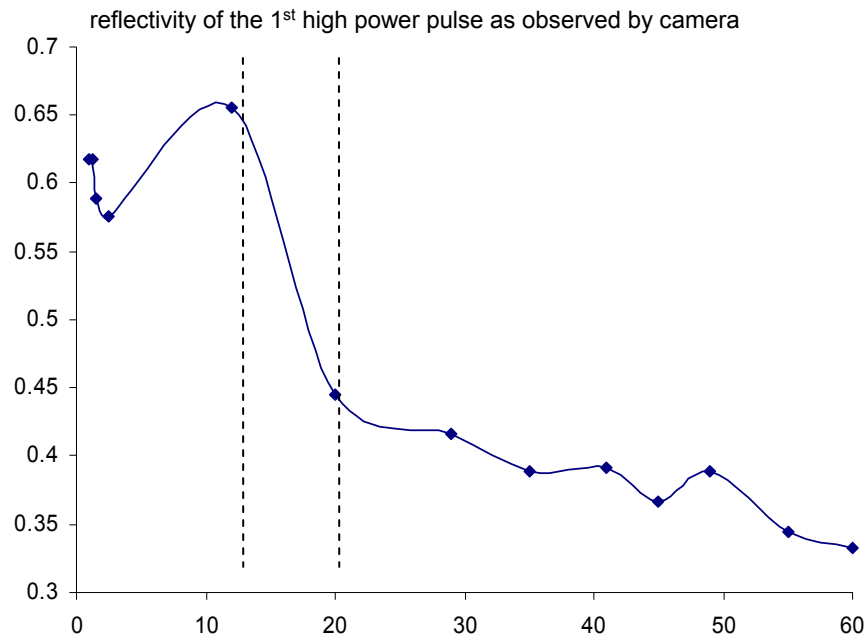

Low power reflected beam

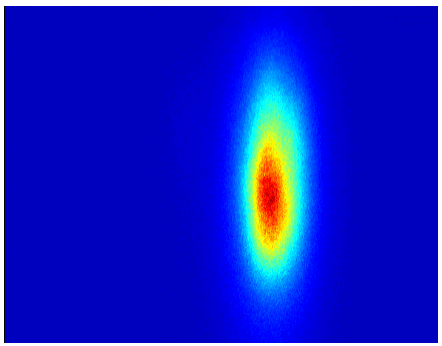

High power reflected beam

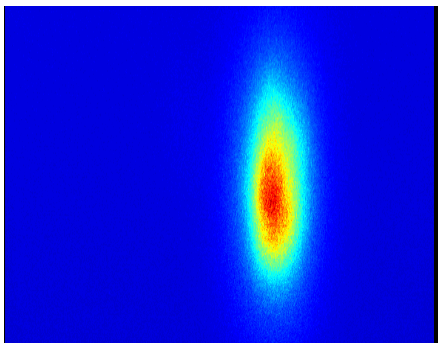

High power reflected beam
2nd laser shot

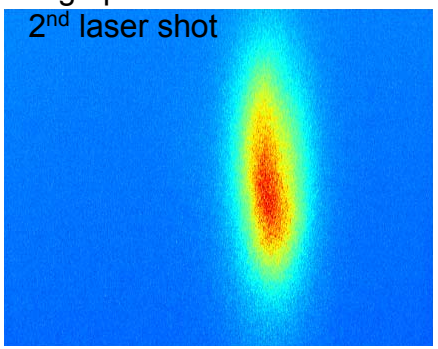

Computation of the energy modulation strength

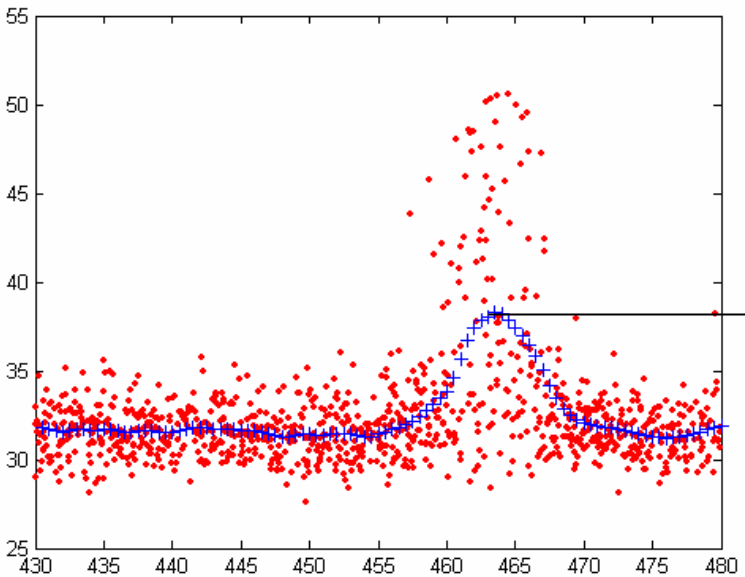

$$QD = \sqrt{(\mathrm{FWHM}_{\mathrm{ON}})^2 - (\mathrm{FWHM}_{\mathrm{OFF}})^2}$$

averaged

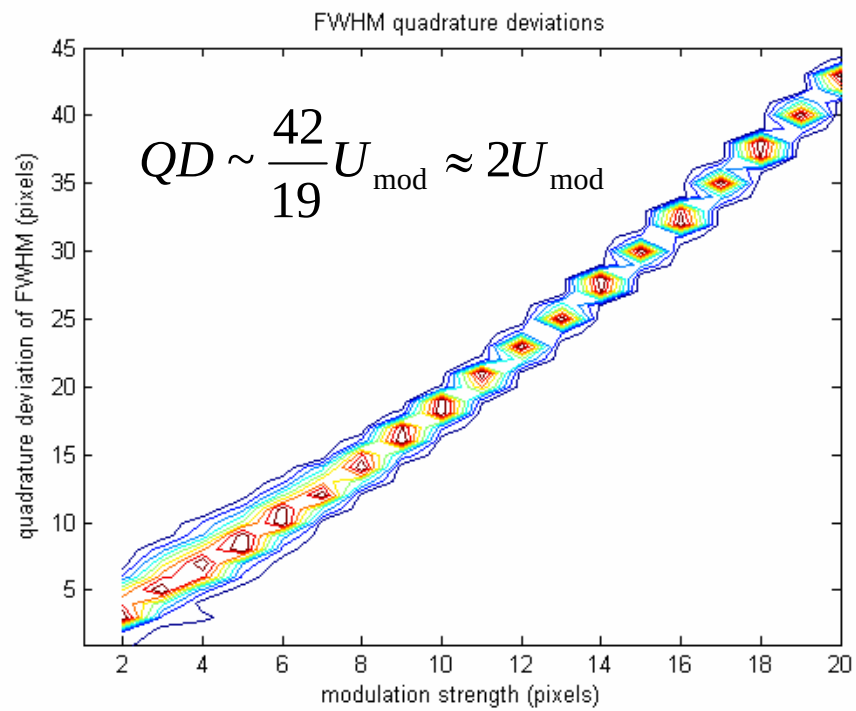

$$QD \sim \frac{42}{19} U_{\mathrm{mod}} \approx 2U_{\mathrm{mod}}$$